Endothelial sulfonylurea receptor 1–regulated $NC_{Ca\text{-}ATP}$ channels mediate progressive hemorrhagic necrosis following spinal cord injury

J. Marc Simard,[1,2,3] Orest Tsymbalyuk,[1] Alexander Ivanov,[1] Svetlana Ivanova,[1] Sergei Bhatta,[1] Zhihua Geng,[1] S. Kyoon Woo,[1] and Volodymyr Gerzanich[1]

[1]Department of Neurosurgery, [2]Department of Pathology, and
[3]Department of Physiology, School of Medicine, University of Maryland at Baltimore, Baltimore, Maryland, USA.

Acute spinal cord injury (SCI) causes progressive hemorrhagic necrosis (PHN), a poorly understood pathological process characterized by hemorrhage and necrosis that leads to devastating loss of spinal cord tissue, cystic cavitation of the cord, and debilitating neurological dysfunction. Using a rodent model of severe cervical SCI, we tested the hypothesis that sulfonylurea receptor 1–regulated (SUR1-regulated) Ca^{2+}-activated, $[ATP]_i$-sensitive nonspecific cation ($NC_{Ca\text{-}ATP}$) channels are involved in PHN. In control rats, SCI caused a progressively expansive lesion with fragmentation of capillaries, hemorrhage that doubled in volume over 12 hours, tissue necrosis, and severe neurological dysfunction. SUR1 expression was upregulated in capillaries and neurons surrounding necrotic lesions. Patch clamp of cultured endothelial cells exposed to hypoxia showed that upregulation of SUR1 was associated with expression of functional SUR1-regulated $NC_{Ca\text{-}ATP}$ channels. Following SCI, block of SUR1 by glibenclamide or repaglinide or suppression of *Abcc8*, which encodes for SUR1 by phosphorothioated antisense oligodeoxynucleotide essentially eliminated capillary fragmentation and progressive accumulation of blood, was associated with significant sparing of white matter tracts and a 3-fold reduction in lesion volume, and resulted in marked neurobehavioral functional improvement compared with controls. We conclude that SUR1-regulated $NC_{Ca\text{-}ATP}$ channels in capillary endothelium are critical to development of PHN and constitute a major target for therapy in SCI.

Introduction

Acute spinal cord injury (SCI) results in physical disruption of spinal cord neurons and axons leading to deficits in motor, sensory, and autonomic function. SCI is a debilitating neurological disorder common in young adults that often requires lifelong therapy and rehabilitative care, placing significant burdens on health care systems. Although many patients exhibit neuropathologically and clinically complete cord injuries following SCI, many others have neuropathologically incomplete lesions (1, 2), giving hope that proper treatment to minimize secondary injury may reduce the functional impact of SCI.

The concept of secondary injury in SCI arises from the observation that the lesion expands and evolves over time (2, 3). Whereas primary injured tissues are irrevocably damaged at the time of impact, tissues that are destined to become secondarily injured are considered to be potentially salvageable. Older observations, based on histological studies, that gave rise to the concept of lesion evolution have been confirmed with noninvasive MRI (4).

Several mechanisms of secondary injury have been postulated, including ischemia/hypoxia, oxidative stress, and inflammation, all of which have been considered to be responsible for the devastating process of progressive hemorrhagic necrosis (PHN) (2, 5–9). PHN is a mysterious condition, first recognized over 3 decades ago, that has thus far eluded understanding and treatment. Shortly after injury (10–15 min), a small hemorrhagic lesion involving primarily the capillary-rich central gray matter is observed, but over the following 3–24 hours, petechial hemorrhages emerge in more distant tissues, eventually coalescing into the characteristic lesion of hemorrhagic necrosis (10, 11). The white matter surrounding the hemorrhagic gray matter shows a variety of abnormalities, including decreased H&E staining, disrupted myelin, and axonal and periaxonal swelling. White matter lesions extend far from the injury site, especially in the posterior columns (8). The evolution of hemorrhage and necrosis has been referred to as "autodestruction." PHN results in loss of vital spinal cord tissue and, in some species, including humans, leads to post-traumatic cystic cavitation surrounded by glial scar tissue.

The mechanism responsible for PHN is not known. Tator and Koyanagi (8) speculated that obstruction of small intramedullary vessels by the initial mechanical stress or secondary injury might be responsible for PHN, whereas Kawata and colleagues (11) attributed the progressive changes to leukocyte infiltration around the injured area leading to plugging of capillaries. Given that petechial hemorrhages, the pathognomonic feature of PHN, form as a result of catastrophic failure of vascular integrity, damage to the endothelium of spinal cord capillaries and postcapillary venules has long

Nonstandard abbreviations used: ODN, oligodeoxynucleotide; $NC_{Ca\text{-}ATP}$, Ca^{2+}-activated, $[ATP]_i$-sensitive nonspecific cation (channel); PHN, progressive hemorrhagic necrosis; SCI, spinal cord injury; SUR1, sulfonylurea receptor 1.

Conflict of interest: J.M. Simard has applied for a US patent, "A novel non-selective cation channel in neural cells and methods for treating brain swelling" (application no. 10/391,561). The remaining authors have declared that no conflict of interest exists.

Citation for this article: *J. Clin. Invest.* **117**:2105–2113 (2007). doi:10.1172/JCI32041.

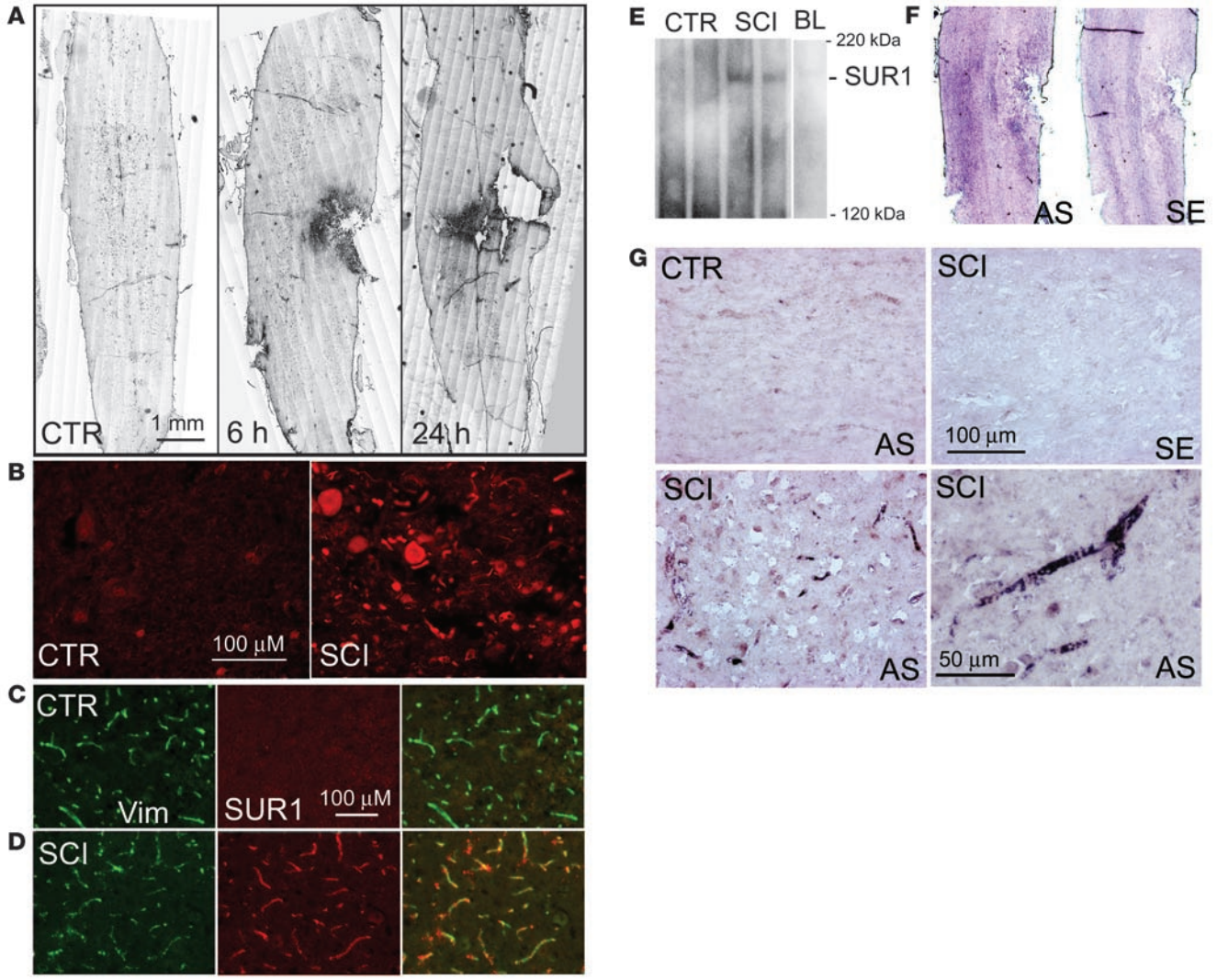

Figure 1

SUR1 is upregulated in SCI. (**A**) Immunohistochemical localization of SUR1 in control rats (CTR) and at different times after SCI as indicated, with montages constructed from multiple individual images and positive labeling shown in black pseudocolor. (**B**) Magnified views of SUR1-immunolabeled sections taken from control and from the core (heavily labeled area in **A** at 6 hours). (**C** and **D**) Immunolabeling of capillaries with vimentin (Vim) and colabeling with SUR1 in control rats (**C**) and from the penumbra of SCI rats (tissue adjacent to the heavily labeled core in **A**, 6 hours) (**D**). (**E**) Western blots for SUR1 of spinal cord tissue from control rats (50 μg protein), from rats 6 hours after SCI (50 μg protein), and from an equivalent amount of blood (BL; 2 μl) as is present in the injured cord. Blots are representative of 5–6 control and SCI rats. (**F** and **G**) In situ hybridization for *Abcc8* in control rats and in whole cords (**F**) or in the penumbra (**G**) 6 hours after SCI using antisense (AS) and sense (SE) as indicated. Immunohistochemistry and in situ hybridization images are representative of findings in 3–5 rats per group. Scale bars: 1 mm (**A**); 100 μM (**B**–**D** and **G**, top panels and bottom left panel); 50 μM (**G**, bottom right panel).

been regarded as a major factor in the pathogenesis of PHN (5, 12, 13). However, to our knowledge, no molecular mechanism for progressive dysfunction of endothelium has yet been identified.

The sulfonylurea receptor 1–regulated (SUR1-regulated) Ca^{2+}-activated, $[ATP]_i$-sensitive nonspecific cation ($NC_{Ca\text{-}ATP}$) channel is a nonselective cation channel that is not constitutively expressed, but is transcriptionally upregulated in astrocytes and neurons following hypoxic or ischemic insult (14–16). The channel is inactive when expressed but becomes activated when intracellular ATP is depleted, with activation leading to cell depolarization, cytotoxic edema, and oncotic cell death. Block of the channel in vitro by the sulfonylurea glibenclamide prevents cell depolarization, cytotoxic edema, and oncotic cell death induced by ATP depletion. In rodent models of ischemic stroke, treatment with glibenclamide results in significant improvements in edema, lesion volume, and mortality (16). In humans with diabetes mellitus, use of sulfonylureas before and during hospitalization for stroke is associated with significantly better stroke outcomes (17).

We hypothesized that $NC_{Ca\text{-}ATP}$ channels might also be involved in PHN in SCI. Although endothelial dysfunction has been implicated in PHN, SUR1-regulated $NC_{Ca\text{-}ATP}$ channels have not previously been shown to our knowledge in capillary endothelium. Here, we used a rodent model of unilateral cervical SCI and endothelial cell cultures to evaluate our hypothesis. We found

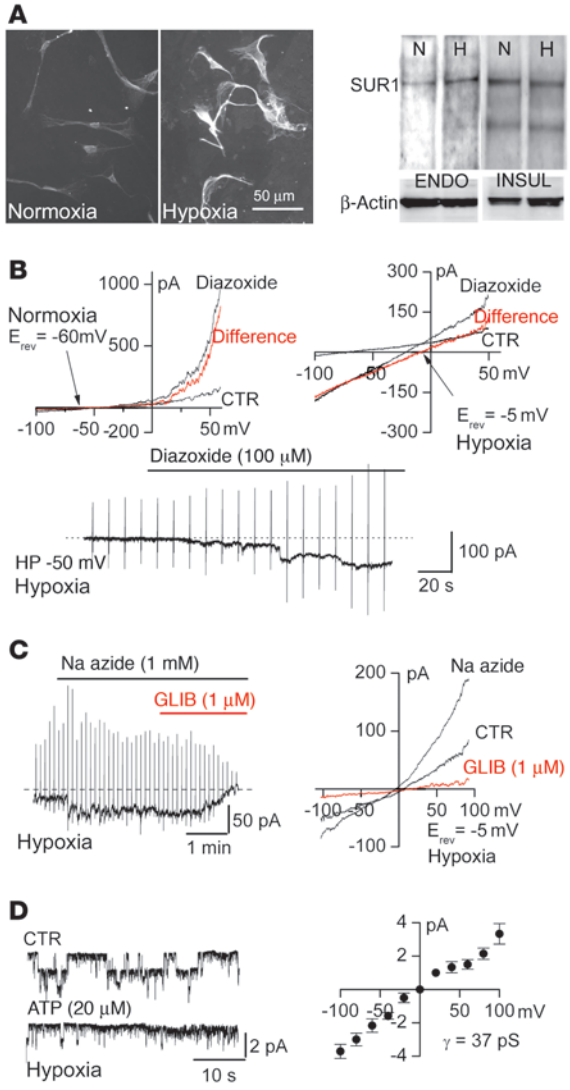

Figure 2
The SUR1-regulated $NC_{Ca\text{-}ATP}$ channel is upregulated in endothelial cells by hypoxia. (**A**) Immunolabeling (scale bar: 50 μm) and Western blots for SUR1 in human aortic endothelial cells (ENDO) cultured under normoxic (N) or hypoxic (H) conditions as indicated, as well as Western blots for SUR1 of rat insulinoma RIN-m5F cells (INSUL) cultured under normoxic or hypoxic condition, with β-actin also shown. (**B** and **C**) Whole-cell currents during ramp pulses (4 per minute; holding potential [HP], –50 mV) or at the holding potential of –50 mV, before and after application of diazoxide (**B**) or Na azide (**C**), in endothelial cells exposed to normoxic or hypoxic conditions; the difference currents are also shown in red. E_{rev}, reversal potential; GLIB, glibenclamide. Data are representative of 7–15 recordings from human aortic endothelial cells (**B**) or bEnd.3 cells (**C**) for each condition. (**D**) Single-channel recordings of inside-out patches with Cs^+ as the principal cation, with channel openings inhibited by ATP on the cytoplasmic side; channel amplitude at various potentials indicated a slope conductance of 37 pS (data from 7 patches) from human brain microvascular endothelial cells. Error bars indicate SEM.

that SUR1 was prominently upregulated in capillaries in the region of SCI in rats; that endothelial cells subjected to hypoxic conditions express SUR1-regulated $NC_{Ca\text{-}ATP}$ channels; and that inhibition of SUR1 by a variety of molecularly distinct mechanisms largely eliminated the progressive extravasation of blood characteristic of PHN, reduced lesion size, and was associated with marked neurobehavioral functional improvement. These findings are all consistent with a critical role for SUR1-regulated $NC_{Ca\text{-}ATP}$ channels in PHN following SCI.

Results

Upregulation of SUR1 in SCI. We studied SUR1 expression in spinal cords of uninjured rats and rats after severe SCI (10-g weight dropped from a 25-mm height; n = 3–5 per group) (18, 19). In controls, low levels of SUR1 expression were found in the dorsal horns (Figure 1A) as a result of constitutively expressed K_{ATP} channels (20).

After unilateral SCI, the lesion itself as well as the pattern of SUR1 expression changed with time and distance from the impact site (Figure 1A). Early after SCI (45 minutes), the lesion was small and was not immunolabeled by anti-SUR1 antibody (data not shown). At 6 hours, a necrotic lesion was apparent as a void in the ipsilateral cord, and SUR1 upregulation was prominent in tissues surrounding the void. At 24 hours, as the necrotic lesion had enlarged (5, 21), SUR1 upregulation was still apparent in the rim of the necrotic lesion, but extended to tissues more distant from the impact site, including into the contralateral hemicord. Immunolabeling for SUR2 was detected only in vascular smooth muscle cells of pial arterioles, both before and after SCI (data not shown).

In the core of the lesion (heavily labeled area in Figure 1A, center), SUR1 upregulation was present in various cells and structures, including large ballooned neuron-like cells and capillary-like elongated structures (Figure 1B). In the penumbra (tissue adjacent to the lesion core), SUR1 upregulation was associated predominantly with capillaries (Figure 1, C and D).

Upregulation of SUR1 was confirmed with immunoblots. With the amount of protein loaded, SUR1 was not detectable in normal cords, whereas a prominent single band at about 190 kDa (16) was observed 6 hours after SCI (Figure 1E). The blood introduced into the tissues by the injury did not account for the increase in SUR1 (Figure 1E). In situ hybridization confirmed widespread expression of *Abcc8*, which encoded for SUR1, after injury, especially in capillaries and postcapillary venules in the penumbra (Figure 1, F and G).

SUR1 in endothelium is associated with the $NC_{Ca\text{-}ATP}$ channel. SUR1 forms the regulatory subunit of $NC_{Ca\text{-}ATP}$ channels and some K_{ATP} channels (15). Our previous work demonstrated that following exposure to hypoxia or ischemia in vivo, upregulation of SUR1 in astrocytes and neurons is associated with expression of functional $NC_{Ca\text{-}ATP}$ channels, not K_{ATP} channels (15, 16). The same reports also showed upregulation of SUR1 in capillaries, as we found here with SCI, but the associated channel was not identified. Endothelial cells may normally express K_{ATP} channels, but the regulatory subunit of cardiovascular K_{ATP} channels is generally SUR2, not SUR1 (22). Nevertheless, it was important to determine with which of the 2 channels, K_{ATP} or $NC_{Ca\text{-}ATP}$, the newly expressed SUR1 was associated in capillary endothelium.

Endothelial cell cultures from 3 sources — human brain microvascular, human aorta, and murine brain microvascular — were used to assess SUR1 expression and characterize channel properties following exposure to hypoxia, with the same results observed for all 3 cultures. Control cultures showed little expression of SUR1, but exposure to hypoxia for 24 hours caused substantial upregulation of SUR1 (Figure 2A). Insulinoma cells, which constitutively express

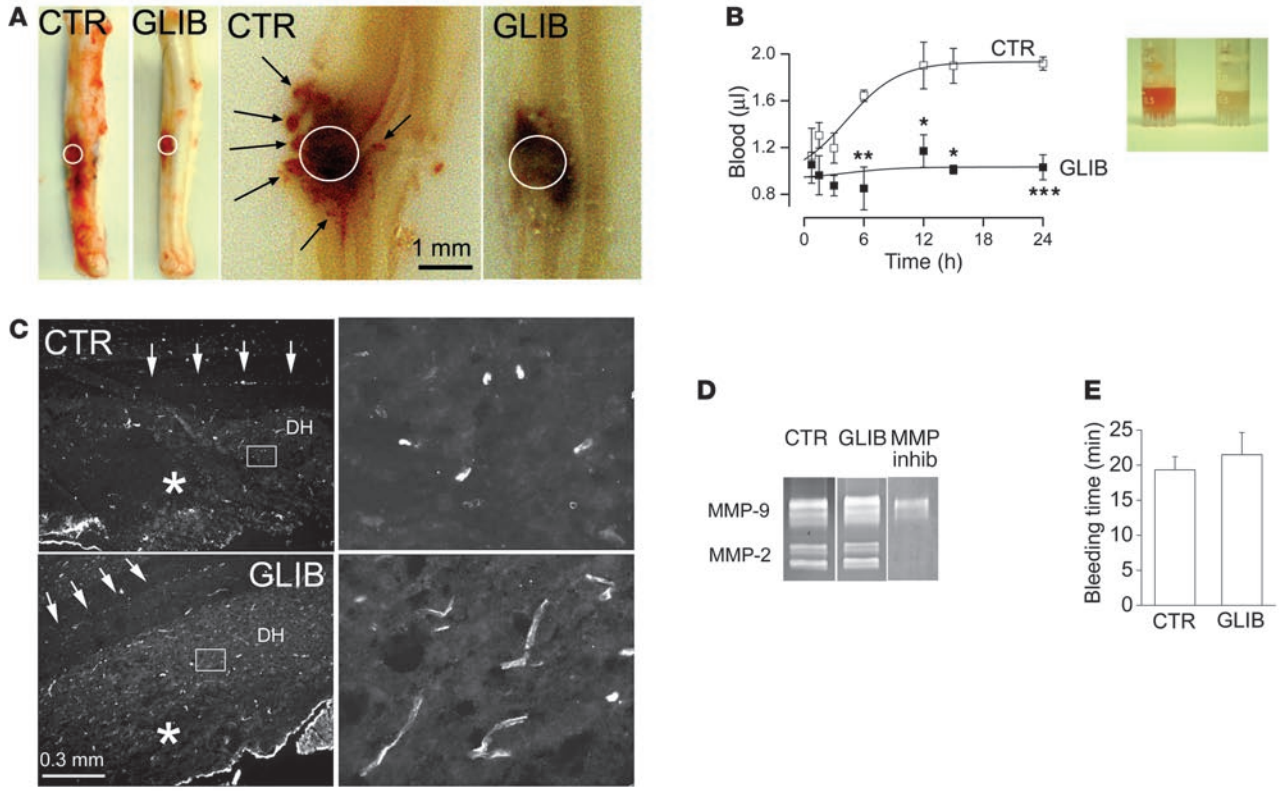

Figure 3
Block of SUR1 reduces hemorrhage after SCI. (**A**) Whole cords and longitudinal sections of cords 24 hours after SCI, from vehicle-treated control and glibenclamide-treated rats. White circles indicate site of impact; arrows denote petechial hemorrhages. (**B**) Cord homogenates in test tubes at 24 hours (inset) and spectrophotometric measurements of blood in cord homogenates at various times after SCI from vehicle-treated ($n = 66$) and glibenclamide-treated ($n = 62$) rats. $^*P < 0.05$, $^{**}P < 0.01$, $^{***}P < 0.001$ versus control. (**C**) Cord sections immunolabeled for vimentin to show capillaries from SCI rats treated with vehicle or glibenclamide; arrows indicate the central canal. Right panels are higher-magnification images of boxed areas in left panels. Images are representative of findings in 6 rats per group. Asterisks indicate lesion core at impact site. DH, dorsal horn. (**D**) Zymography of recombinant MMP-2 and MMP-9 performed under control conditions, in the presence of glibenclamide (10 μM), and in the presence of MMP inhibitor II (MMP inhib; 300 nM). (**E**) Bleeding times in uninjured rats infused with vehicle or glibenclamide ($n = 3$ per group). Error bars indicate SEM. Scale bars: 1 mm (**A**); 0.3 mm (**C**, left panels). Original magnification, ×40 (**C**, right panels).

SUR1-regulated K_{ATP} channels, showed no upregulation of SUR1 when exposed to the same hypoxic conditions (Figure 2A).

Patch clamp of endothelial cells was performed using a nystatin-perforated patch technique in order to maintain the metabolic integrity of the cells. The identity of the activated channel can be assessed by measurement of the reversal potential, the potential at which an ion channel current reverses from inward to outward. With physiologically relevant concentrations of ions intracellularly and extracellularly (high K inside, high Na outside), the reversal potential can unambiguously distinguish between a K^+ channel current such as K_{ATP}, which reverses at a potential negative to –50 mV, and a nonselective cation channel current such as $NC_{Ca\text{-}ATP}$, which reverses near 0 mV.

We studied channel activation by diazoxide, which opens SUR-regulated channels without ATP depletion and, of SUR activators, is the most selective for SUR1 over SUR2 (15). Patch clamp of endothelial cells cultured under normoxic conditions showed that diazoxide had no effect or, in half of the cells, activated an outwardly rectifying current that reversed at potentials more negative than –50 mV, consistent with a K_{ATP} channel (Figure 2B) (23). By contrast, in most endothelial cells cultured under hypoxic conditions, diazoxide activated an ohmic current that reversed near 0 mV and was inward at –50 mV (Figure 2B), which is incompatible with K_{ATP}, but consistent with $NC_{Ca\text{-}ATP}$ channels (14–16).

We also studied channel activation induced by Na azide, a mitochondrial uncoupler that depletes cellular ATP (14). In most endothelial cells exposed to hypoxic conditions, Na azide–induced ATP depletion activated an ohmic current that was inward at –50 mV, reversed near 0 mV, and was blocked by 1 μM glibenclamide (Figure 2C), again consistent with $NC_{Ca\text{-}ATP}$ channels.

Single-channel recordings were performed using inside-out patches, with Cs^+ as the only permeant cation. This confirmed the presence of a channel that was sensitive to block by ATP on the cytoplasmic side and that had a single channel conductance of 37 pS (Figure 2D). These findings are incompatible with K_{ATP} channels, which are not permeable to Cs^+ and have slope conductance of ~75 pS, but are consistent with $NC_{Ca\text{-}ATP}$ channels.

The characteristics of the channel identified in endothelial cells from both aorta and brain capillaries from 2 species — including expression only after exposure to hypoxia, activation by depletion of cellular ATP or diazoxide, a reversal potential near 0 mV, conductance of Cs^+, and single channel conductance of 37 pS —

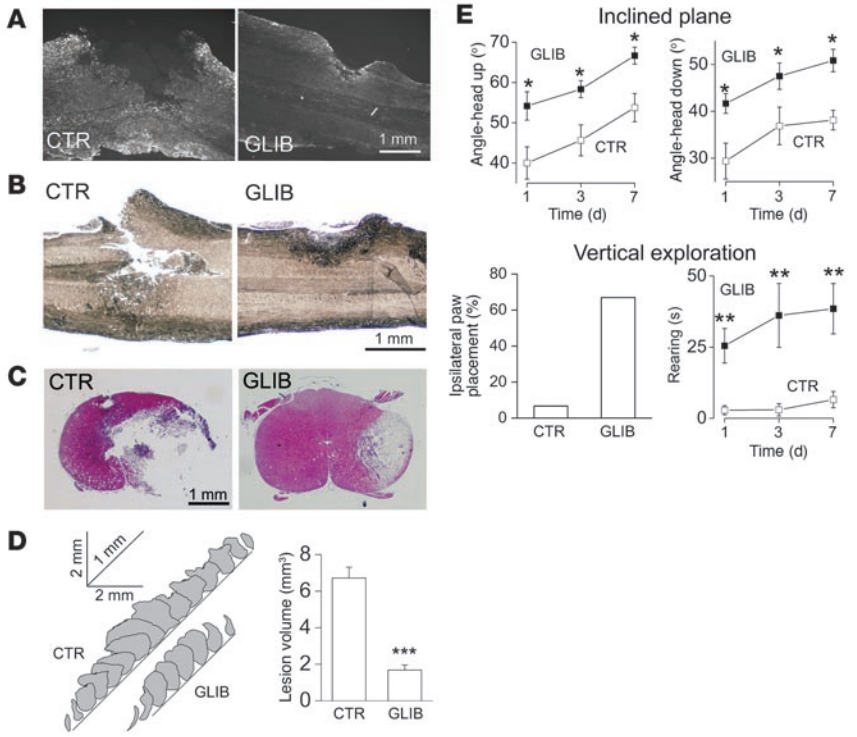

Figure 4
Blocking SUR1 reduces lesion size and improves neurobehavioral function after SCI. (**A**–**C**) Cord sections immunolabeled for glial fibrillary acidic protein (**A**) or stained with eriochrome cyanine R (**B**) or H&E (**C**), 1 day (**A** and **B**) or 7 days (**C**) after SCI, from vehicle-treated and glibenclamide-treated rats. Images are representative of findings in 3 rats per group. Scale bars: 1 mm. (**D**) Cascaded outlines of lesion areas in serial sections 250 μm apart, 7 days after SCI, as well as lesion volumes from vehicle-treated and glibenclamide-treated rats (n = 4–6 per group; excludes 2 control rats that died). (**E**) Performance on inclined plane (head up and head down), ipsilateral paw placement, and rearing in the same vehicle-treated and glibenclamide-treated rats as in **D**. Paw placement was measured 1 day after SCI. Error bars indicate SEM. *P < 0.05, **P < 0.01, ***P < 0.001 versus control.

reproduce exactly our previous findings with $NC_{Ca\text{-}ATP}$ channels in astrocytes and neurons (14–16) and reaffirm that the $NC_{Ca\text{-}ATP}$ channel is not constitutively expressed, is upregulated only with an appropriate insult, and, when expressed, is inactive until intracellular ATP is depleted.

Glibenclamide block of SUR1: extravasation of blood. To assess the role of SUR1 in SCI, we studied the effect of glibenclamide, a sulfonylurea inhibitor that binds with subnanomolar or nanomolar affinity (0.4–4.0 nM) to SUR1 (24). Immediately after injury, animals were implanted with mini-osmotic pumps that delivered either vehicle or glibenclamide (200 ng/h) s.c. We used constant infusion of a low dose of drug to achieve sustained occupancy of only high-affinity receptors.

Cords of vehicle-treated animals examined 24 hours after SCI showed prominent bleeding at the surface and internally, with internal bleeding consisting of a central region of hemorrhage plus numerous distinct petechial hemorrhages at the periphery (Figure 3A, arrows). By contrast, cords of glibenclamide-treated animals showed visibly less hemorrhage, and it was largely confined to the site of impact, with fewer petechial hemorrhages in surrounding tissues (Figure 3A).

We quantified the amount of extravasated blood in tissue homogenates at different times after SCI, after first removing intravascular blood (Figure 3B). In cords from vehicle-treated animals, measurements showed a progressive increase in the amount of blood, with a maximum reached about 12 hours after SCI (Figure 3B). By contrast, cords from glibenclamide-treated animals showed little increase in extravasated blood during the 24 hours after injury, with most of the blood present at 24 hours attributable to the initial impact (Figure 3B).

Formation of petechial hemorrhages implies catastrophic failure of capillary integrity. We examined capillaries in the region of injury by immunolabeling with vimentin, which is upregulated in endothelium following injury (25). In control animals, vimentin-positive capillaries appeared foreshortened or fragmented, whereas in glibenclamide-treated animals, the capillaries were elongated and appeared more normal (Figure 3C).

In postischemic reperfusion of CNS tissues, catastrophic failure of capillary integrity has been attributed to the action of MMPs (26). We assessed whether glibenclamide might have an effect on MMP activity by using zymography to measure gelatinase activity of recombinant MMP. Gelatinase activity was not affected by glibenclamide, although it was strongly inhibited by a specific MMP inhibitor (Figure 3D), indicating that the reduction in hemorrhage with glibenclamide could not be attributed to MMP inhibition. Glibenclamide did not affect bleeding time (Figure 3E), suggesting that the reduction in hemorrhage with glibenclamide following SCI was unlikely to be the result of an effect on coagulation or platelet function (27). The dose of glibenclamide used caused a small decrease in serum glucose levels, from 236 ± 15 mg/dl to 201 ± 20 mg/dl (n = 5 per group; P = 0.19), measured 3 hours after SCI.

Glibenclamide block of SUR1: lesion size. Labeling of longitudinal sections for the astrocyte marker glial fibrillary acidic protein and for myelin revealed that glibenclamide treatment was associated with smaller lesions, less reactive gliosis, and better myelin preservation 24 hours after SCI compared with controls (Figure 4, A and B). Similarly, H&E staining of cross sections showed that glibenclamide treatment was associated with smaller lesions at 7 days after SCI compared with controls (Figure 4C). In vehicle-treated controls at both 1 and 7 days after SCI, the lesions incorporated large voids of necrotic tissue that involved most of the hemicord ipsilateral to the impact site and typically extended to the contralateral hemicord. White matter tracts of the contralateral hemicord were typically disrupted. By contrast, lesions in glibenclamide-treated animals were smaller and typically did not cross the midline, and contralateral as well as portions of ipsilateral white matter tracts were spared.

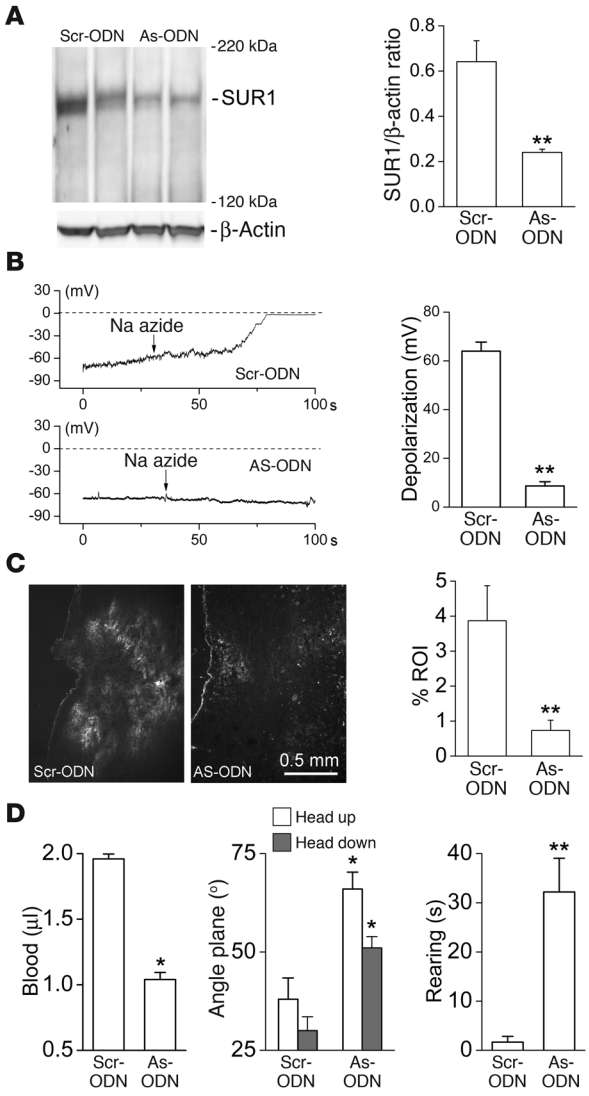

Figure 5
Gene suppression of SUR1 blocks expression of functional $NC_{Ca\text{-}ATP}$ channels and improves outcome in SCI. (**A**) Western blots for SUR1 in gliotic capsule from rats with infusion of scrambled ODN (Scr-ODN) or antisense ODN (AS-ODN) directly into the brain injury site for 10–12 days prior to tissue harvest. Also shown is densitometric analysis of Western blots from the same groups of rats ($n = 3$ per group). (**B**) Membrane potential of astrocytes from gliotic capsules of the same groups of rats as in **A** during application of Na azide to deplete ATP. Mean depolarization of 3 cells per group is shown. (**C**) Cord sections immunolabeled for SUR1, 1 day after SCI, from rats treated with i.v. infusion of scrambled ODN or antisense ODN. Scale bar: 0.5 mm. Also shown is quantitative immunofluorescence for the same groups of rats ($n = 3$ per group). ROI, region of interest. (**D**) Blood in cord homogenates, performance on angled plane, and rearing, 1 day after SCI, for rats treated with i.v. infusion of scrambled ODN or antisense ODN. Error bars indicate SEM. $^*P < 0.05$, $^{**}P < 0.01$ versus scrambled ODN.

Lesion volumes at 7 days were approximately 3-fold smaller in glibenclamide-treated rats compared with controls (Figure 4D). Notably, the lesion volumes we observed with glibenclamide treatment following severe impact were comparable to those observed by other investigators in untreated rats using the same cervical contusion model following mild impact (10-g weight dropped from a 6.25-mm height; ref. 19).

Glibenclamide block of SUR1: neurobehavioral function. Vehicle-treated rats were generally not mobile (18), whereas glibenclamide-treated rats were typically ambulatory and often exhibited proficient exploratory behavior. When suspended by their tails, vehicle-treated rats hung passively with little or no flexion of the trunk, whereas glibenclamide-treated rats could typically flex their trunks, bringing the snout to the level of the thorax or hindquarters.

We tested the same animals used to assess lesion size on an inclined plane, a standard test that requires more and more dexterous function of the limbs and paws as the angle of the plane is increased (28). At 1, 3, and 7 days after SCI, glibenclamide treatment was associated with significantly better performance than vehicle treatment (Figure 4E). We also quantified ipsilateral paw placement, which is characteristically lost following cervical hemicord transection (29). In the same animals tested 1 day after SCI, glibenclamide treatment was associated with significantly better performance than vehicle treatment (Figure 4E).

The Basso, Beattie, Bresnahan scale (BBB scale; ref. 30) is commonly used to evaluate neurobehavioral function in rodents after SCI. However, it was designed for thoracic-level lesions, not cervical-level lesions, and the highest level of performance that it records is less than what our glibenclamide-treated rats could achieve. We therefore quantified vertical exploratory behavior (referred to herein as rearing), a complex exercise that requires balance, truncal stability, bilateral hind limb dexterity, and strength, and at least unilateral fore limb dexterity and strength, which together are excellent markers of cervical spinal cord function. Testing the same rats as above at 1, 3, and 7 days after SCI showed that glibenclamide treatment was associated with significantly better performance than vehicle treatment (Figure 4E). In additional groups of rats tested only at 1 day after SCI, similar differences were observed (3 ± 1 s versus 42 ± 7 s; $P = 0.001$; $n = 14$–15 per group).

Repaglinide block of SUR1. Repaglinide is a member of a distinct class of insulin secretagogues that are structurally unrelated to sulfonylureas and whose binding site may differ from that of a sulfonylurea (31). Like glibenclamide, repaglinide produces high-affinity block of both native and recombinant β cell K_{ATP} channels (IC_{50}, 0.9–7 nM) and shows higher potency in inhibiting pancreatic SUR1-regulated K_{ATP} channels than in inhibiting cardiovascular SUR2-regulated channels (32). We examined the effect of repaglinide on PHN, using the same treatment regimen as used for glibenclamide. As with glibenclamide, repaglinide treatment reduced blood in cord homogenates from 1.8 ± 0.2 μl to 1.2 ± 0.1 μl at 1 day after SCI ($P < 0.01$; $n = 5$–8 per group) and was associated with significantly better performance than vehicle-treated controls on the inclined plane (head up, $40 \pm 4°$ versus $62 \pm 2°$, $P = 0.01$; head down, $29 \pm 4°$ versus $47 \pm 3°$, $P = 0.03$; $n = 3$–8 per group) and in rearing (3 ± 2 s versus 27 ± 6 s; $P = 0.005$; $n = 5$–6 per group).

Gene suppression of SUR1. We used gene suppression to confirm involvement of SUR1 in PHN, choosing an antisense oligodeoxynucleotide (ODN) strategy shown to be effective in vitro (33). To validate the antisense strategy, we first implemented it in the model that we previously used for the discovery of the $NC_{Ca\text{-}ATP}$ channel, in which a gelatin sponge is implanted into the parietal lobe to stimulate formation of a gliotic capsule (14). Here, animals were also fitted with mini-osmotic pumps that delivered ODNs, either antisense or scrambled, continuously for 7 days

into the injury site. Gliotic capsules from rats treated with antisense ODN showed a significant reduction in SUR1 protein compared with scrambled ODN–treated rats (Figure 5A). Patch clamp of astrocytes from gliotic capsule of rats treated with scrambled ODN showed that they rapidly depolarized when cellular ATP was depleted by exposure to Na azide (Figure 5B), an effect that we previously showed was caused by the opening of $NC_{Ca\text{-}ATP}$ channels (15). By contrast, astrocytes from rats treated with antisense ODN depolarized slightly or not at all (Figure 5B), demonstrating that SUR1 is required for expression of functional $NC_{Ca\text{-}ATP}$ channels, just as with K_{ATP} channels (34).

For experiments with SCI, we used antisense ODNs and scrambled ODNs that were phosphorothioated at 4 distal bonds to protect against endogenous nucleases (35); ODNs were administered i.v. starting immediately after injury. At 6 hours after SCI, cords from rats treated with antisense ODN showed significantly less immunolabeling for SUR1 than did controls (Figure 5C). With scrambled ODN, the necrotic void beneath the impact site was surrounded by an SUR1-positive shell of tissue, similar to our observations in untreated animals (Figure 1A). With antisense ODN, however, only the small volume of tissue immediately beneath the impact site was labeled for SUR1, and no necrotic void was evident (Figure 5C). Antisense ODN did not affect normal expression of SUR1 in dorsal horn cells (Figure 5C). At 1 day after SCI, treatment with antisense ODN reduced blood in cord homogenates and was associated with significantly better performance on the inclined plane and in rearing compared with scrambled ODN treatment (Figure 5D).

Discussion

Here, we report what we believe to be the novel findings that SUR1 is strongly upregulated following SCI and that block of SUR1 is associated with significant improvements in all of the characteristic manifestations of PHN, including hemorrhage, tissue necrosis, lesion evolution, and neurological dysfunction. Although our focus in this report was on SUR1 and $NC_{Ca\text{-}ATP}$ channels in capillary endothelium, our data also showed early (<6 h) upregulation of SUR1 in large neuron-like cells in the core near the impact site, and in other experiments, we observed late (12–24 h) upregulation of SUR1 in reactive astrocytes (our unpublished observations). These responses to SCI may be compared with findings we previously reported for ischemic stroke, in which there is early upregulation of SUR1 in neurons and capillaries in the core and later upregulation of SUR1 in capillaries and astrocytes in penumbral tissues (16).

PHN has been linked to tissue ischemia (5, 21), but to our knowledge, it has not previously been characterized at a molecular level. PHN is probably a variant of hemorrhagic conversion, a mechanism of secondary injury in the CNS, wherein capillaries or postcapillary venules undergo delayed catastrophic failure that allows extravasation of blood to form petechial hemorrhages, which in turn coalesce into a unified region of hemorrhagic necrosis or infarction (36). Hemorrhagic conversion is common in traumatic brain injury (37) and following postischemic reperfusion (26), with hypoxia and active perfusion being important antecedents (36). The molecular pathology involved in hemorrhagic conversion has not been fully elucidated, but work in ischemic stroke has implicated enzymatic destruction of capillaries by MMPs (26, 38). MMPs have been implicated in SCI (39, 40), but not in PHN.

The work reported here implicates endothelial SUR1-regulated $NC_{Ca\text{-}ATP}$ channels in PHN. Our data show that PHN was associated with upregulation of SUR1 in capillaries and postcapillary venules, structures long held to be responsible for PHN (12, 13). Moreover, our data show that block of SUR1 by 3 molecularly distinct agents, glibenclamide, repaglinide, and antisense ODN, significantly reduced PHN. The remarkably similar outcomes obtained with highly selective agents that act via distinct molecular mechanisms underscore the important role of SUR1. These data also provide evidence that de novo expression of SUR1 is necessary and sufficient for development of PHN. Use of a knockdown strategy using antisense ODN appears to have been more informative than a gene-knockout strategy, because the latter would not have distinguished between constitutive and de novo expression of SUR1.

SUR1 forms the regulatory subunit of $NC_{Ca\text{-}ATP}$ channels and some K_{ATP} channels (15, 16). Here, we showed that upregulation of SUR1 in endothelial cells was associated with expression of functional $NC_{Ca\text{-}ATP}$ channels, which we previously implicated in edema formation and cell death in CNS ischemia/hypoxia (16, 36). Our patch-clamp recordings confirmed the presence of a nonselective cation channel that was activated by diazoxide and ATP depletion, blocked by glibenclamide and cytoplasmic ATP, conducted Cs^+, and had a single channel conductance of about 35 pS, all of which are characteristic of the $NC_{Ca\text{-}ATP}$ channel (14, 15). We previously showed that this channel conducts only monovalent cations, not divalent cations (14), but this was not tested here. The experiments reported here showing upregulation of functional $NC_{Ca\text{-}ATP}$ channels were performed using endothelial cells from CNS as well as non-CNS sources from 2 species suggesting a certain degree of generality of the phenomenon. In our patch-clamp experiments, we did not explicitly study endothelial cells from the spinal cord, which could potentially differ from those in the brain. However, it seems unlikely that the upregulation of SUR1 in spinal cord capillaries that we observed was associated with a different channel, such as K_{ATP}. Sulfonylurea block of K_{ATP} would not be expected to be neuroprotective (41), whereas block of $NC_{Ca\text{-}ATP}$ is highly neuroprotective in both rodents and humans (16, 17).

Of the numerous treatments assessed in SCI, few have been shown to actually decrease the hemorrhage and tissue loss associated with PHN. Methylprednisolone, the only approved therapy for SCI, improves edema but does not alter the development of PHN (42). A number of compounds have shown beneficial effects related to tissue sparing, including the *N*-methyl-D-aspartic acid antagonist MK801 (43), the α-amino-3-hydroxy-5-methyl-4-isoxazole propionic acid antagonist GYKI 52466 (44), Na^+ channel blockers (45), and minocycline (46). Overall, to our knowledge no treatment has been reported that reduces PHN and lesion volume and improves neurobehavioral function to the extent observed here with glibenclamide, repaglinide, and antisense ODN.

There are 2 mechanisms by which glibenclamide can antagonize SUR1-regulated $NC_{Ca\text{-}ATP}$ channels: by blocking the channel once it is expressed and subsequently opened by ATP depletion (15), and by interfering with trafficking of SUR1 to the cell membrane, a process that is required for expression of functional channels (47). Both blockade of open channels (16) and SUR1 binding (48) needed to inhibit the trafficking of SUR1 to the cell membrane, are increased an order of magnitude or more at the low pH of ischemic tissues. Block of open channels, interference with trafficking, or both, coupled with the augmented efficacy imparted by low pH, likely account for the high efficacy of glibenclamide found previously with stroke (16) and here with SCI.

Half of patients with SCI initially present with an incomplete lesion (49), making it important to identify therapeutic strategies

to inhibit secondary injury mechanisms. Glibenclamide has been used safely in humans for several decades for treatment of type 2 diabetes, with no untoward side effects except hypoglycemia, and its continued use immediately after stroke improves outcome in patients with type 2 diabetes (17). The safety of glibenclamide, together with its unique mechanism of action in targeting the capillary failure that leads to PHN, indicate that this drug may be especially attractive for translational use in human SCI.

Methods

SCI injury model. This study was approved by and performed in accordance with the guidelines of the Institutional Animal Care and Use Committee of the University of Maryland at Baltimore. Adult female Long-Evans rats (275–350 g) were anesthetized (60 mg/kg ketamine plus 7.5 mg/kg xylazine i.p.). The dura at C4-5 was exposed via a left hemilaminectomy. A hemicervical spinal cord contusion was created using a blunt-force impactor (1.3-mm impactor head driven by a 10-g weight dropped vertically from a 25-mm height) (18, 19). After SCI, animals were given 10 ml of glucose-free normal saline s.c. Rectal temperature was maintained at approximately 37°C using a servo-controlled warming blanket. Blood gases and serum glucose were determined 10–15 minutes after SCI in control (pO_2, 95 ± 6 mmHg; pCO_2, 46 ± 3 mmHg; pH, 7.33 ± 0.01; glucose, 258 ± 17 mg/dl) and glibenclamide-treated animals (pO_2, 96 ± 7 mmHg; pCO_2, 45 ± 2 mmHg; pH, 7.37 ± 0.01; glucose, 242 ± 14 mg/dl).

Drug delivery. Within 2–3 minutes of SCI induction, mini-osmotic pumps (Alzet 2002, 0.5 μl/h; Durect Corp.) were implanted that delivered either vehicle (saline plus DMSO), glibenclamide (Sigma-Aldrich) in vehicle, or repaglinide (Sigma-Aldrich) in vehicle s.c. During the course of the study, slightly different formulations of drug were used, with the best results obtained using stock solutions made by placing 50 mg (or 25 mg) of drug into 10 ml DMSO and infusion solutions made by placing 400 μl (or 800 μl) stock into 4.6 ml (or 4.2 ml) unbuffered saline (0.9% NaCl) and adjusting the pH to approximately 8.5 using 0.1 N NaOH. Infusion solutions of glibenclamide and repaglinide were delivered at 0.5 μl/h, yielding infusion doses of 200 ng/h.

For in vivo gene suppression of *Abcc8*, we used ODNs that were phosphorothioated at 4 distal bonds to protect against endogenous nucleases (35). Within a few minutes of SCI, mini-osmotic pumps (Alzet 2002, 0.5 μl/h; Durect Corp.) with jugular vein catheters were implanted that delivered either scrambled ODN (5′-TGCCTGAGGCGTGGCTGT-3′) or antisense ODN (5′-GGCCGAGTGGTTCTCGGT-3′) (33) in PBS at a rate of 1 mg/rat/24 h.

Tissue blood. Rats were sacrificed at various times after SCI (n = 5–11 per group) and perfused with heparinized saline to remove intravascular blood, and 5-mm segments of cord encompassing the lesion were homogenized and processed as described previously (50).

Lesion size. At 7 days after SCI, cords were paraffin sectioned and stained with H&E. Lesion volumes were calculated from lesion areas measured on serial sections every 250 μm.

Neurobehavioral assessment. All measurements were performed by evaluators blinded to group. Performance on the inclined plane was evaluated as described previously (28). To assess paw placement and rearing (29), animals were videotaped while in a translucent cylinder (19 × 20 cm). Rearing was quantified as the number of seconds spent with both front paws elevated above shoulder height during a 3-minute period of observation.

Bleeding times. Bleeding times were measured using tail-tip bleeding as described previously (51).

Zymography. Zymography of recombinant MMP-2 and MMP-9 (Sigma-Aldrich) was performed as described previously (52). MMP inhibitor II was from Calbiochem.

Cell culture. Endothelial cell cultures from human brain microvessels and human aorta (ScienCell Research Laboratories) as well as murine brain microvessels (bEnd.3; ATCC) were grown at low density using media and supplements recommended by the suppliers.

Abcc8 knockdown in astrocytes. *Abcc8* knockdown in astrocytes was performed in triplicate by implanting rats with gelatin sponges in the parietal lobe to induce formation of a gliotic capsule containing reactive astrocytes that express the SUR1-regulated $NC_{Ca\text{-}ATP}$ channel (14, 15). At the same time, they were implanted with mini-osmotic pumps (Alzet 2002, 14-day pump; Durect Corp.) placed in the dorsal thoracolumbar region that contained ODN (711 μg/ml delivered at a rate of 0.5 μl/h, yielding 1,500 pmol/d), with the delivery catheter placed directly into the site of the gelatin sponge implant in the brain. Animals were infused with scrambled ODN or antisense ODN as described above but not phosphorothioated. After 10–14 days, the gelatin sponge plus encapsulating gliotic tissues were harvested and processed either for Western immunoblots or to obtain fresh reactive astrocytes for patch-clamp electrophysiology.

Patch-clamp electrophysiology. Patch-clamp electrophysiology for the $NC_{Ca\text{-}ATP}$ channel in this lab has been described previously (14, 15).

Immunohistochemistry. Cryosections were immunolabeled (15, 16) using primary antibodies directed against SUR1 (C-16; diluted 1:200; 1 hour at room temperature, 48 hours at 4°C; Santa Cruz Biotechnology Inc.), SUR2 (H-80; diluted 1:200; 1 hour at room temperature, 48 hours at 4°C; Santa Cruz Biotechnology Inc.), glial fibrillary acidic protein (C-9205; diluted 1:500; Sigma-Aldrich), and vimentin (monoclonal CY3 conjugated; diluted 1:100; Sigma-Aldrich). Quantitative immunofluorescence was performed as described previously (53).

Eriochrome staining. Visualization of myelin was obtained using eriochrome cyanine R (Sigma-Aldrich).

Immunoblots. Immunoblots were prepared using antibodies directed against SUR1. The specificity of the antibody (16) was demonstrated by the results of the knockdown experiments shown in Figure 5.

In situ hybridization. Fresh-frozen cord sections were fixed in 5% formaldehyde for 5 minutes. Digoxigenin-labeled probes (sense, 5′-GCCCGGGCACCCTGCTGGCTCTGTGTGTCCTTCCGCGCCTGGGCATCG-3′) were designed and supplied by GeneDetect, and hybridization was performed according to the manufacturer's protocol.

Statistics. Statistical significance was evaluated using ANOVA. A P value of less than 0.05 was considered significant.

Acknowledgments

This work was supported by grants to J.M. Simard from the Maryland Department of Veterans Affairs; the National Institute of Neurological Disorders and Stroke, NIH (NS048260), the National Heart, Lung, and Blood Institute, NIH (HL082517); and the Christopher and Dana Reeve Foundation.

Received for publication March 6, 2007, and accepted in revised form May 9, 2007.

Address correspondence to: J. Marc Simard, Department of Neurosurgery, 22 S. Greene Street, Suite 12SD, Baltimore, Maryland 21201-1595, USA. Phone: (410) 328-0850; Fax: (410) 328-0756; E-mail: msimard@smail.umaryland.edu.

1. Hayes, K.C., and Kakulas, B.A. 1997. Neuropathology of human spinal cord injury sustained in sports-related activities. *J. Neurotrauma.* **14**:235–248.
2. Tator, C.H., and Fehlings, M.G. 1991. Review of the secondary injury theory of acute spinal cord trauma with emphasis on vascular mechanisms. *J. Neurosurg.* **75**:15–26.
3. Kwon, B.K., Tetzlaff, W., Grauer, J.N., Beiner, J., and Vaccaro, A.R. 2004. Pathophysiology and pharma-

cologic treatment of acute spinal cord injury. *Spine J.* **4**:451–464.
4. Bilgen, M., Abbe, R., Liu, S.J., and Narayana, P.A. 2000. Spatial and temporal evolution of hemorrhage in the hyperacute phase of experimental spinal cord injury: in vivo magnetic resonance imaging. *Magn. Reson. Med.* **43**:594–600.
5. Nelson, E., Gertz, S.D., Rennels, M.L., Ducker, T.B., and Blaumanis, O.R. 1977. Spinal cord injury. The role of vascular damage in the pathogenesis of central hemorrhagic necrosis. *Arch. Neurol.* **34**:332–333.
6. Tator, C.H. 1991. Review of experimental spinal cord injury with emphasis on the local and systemic circulatory effects. *Neurochirurgie.* **37**:291–302.
7. Fitch, M.T., Doller, C., Combs, C.K., Landreth, G.E., and Silver, J. 1999. Cellular and molecular mechanisms of glial scarring and progressive cavitation: in vivo and in vitro analysis of inflammation-induced secondary injury after CNS trauma. *J. Neurosci.* **19**:8182–8198.
8. Tator, C.H., and Koyanagi, I. 1997. Vascular mechanisms in the pathophysiology of human spinal cord injury. *J. Neurosurg.* **86**:483–492.
9. Kraus, K.H. 1996. The pathophysiology of spinal cord injury and its clinical implications. *Semin. Vet. Med. Surg. Small Anim.* **11**:201–207.
10. Balentine, J.D. 1978. Pathology of experimental spinal cord trauma. I. The necrotic lesion as a function of vascular injury. *Lab. Invest.* **39**:236–253.
11. Kawata, K., et al. 1993. Experimental study of acute spinal cord injury: a histopathological study [In Japanese]. *No Shinkei Geka.* **21**:45–51.
12. Griffiths, I.R., Burns, N., and Crawford, A.R. 1978. Early vascular changes in the spinal grey matter following impact injury. *Acta Neuropathol.* **41**:33–39.
13. Kapadia, S.E. 1984. Ultrastructural alterations in blood vessels of the white matter after experimental spinal cord trauma. *J. Neurosurg.* **61**:539–544.
14. Chen, M., and Simard, J.M. 2001. Cell swelling and a nonselective cation channel regulated by internal Ca2+ and ATP in native reactive astrocytes from adult rat brain. *J. Neurosci.* **21**:6512–6521.
15. Chen, M., Dong, Y., and Simard, J.M. 2003. Functional coupling between sulfonylurea receptor type 1 and a nonselective cation channel in reactive astrocytes from adult rat brain. *J. Neurosci.* **23**:8568–8577.
16. Simard, J.M., et al. 2006. Newly expressed SUR1-regulated NC(Ca-ATP) channel mediates cerebral edema after ischemic stroke. *Nat. Med.* **12**:433–440.
17. Kunte, H., et al. 2007. Sulfonylureas improve outcome in patients with type 2 diabetes and acute ischemic stroke. *Stroke.* In press.
18. Soblosky, J.S., Song, J.H., and Dinh, D.H. 2001. Graded unilateral cervical spinal cord injury in the rat: evaluation of forelimb recovery and histological effects. *Behav. Brain Res.* **119**:1–13.
19. Gensel, J.C., et al. 2006. Behavioral and histological characterization of unilateral cervical spinal cord contusion injury in rats. *J. Neurotrauma.* **23**:36–54.
20. Yamashita, S., et al. 1994. Possible presence of the ATP-sensitive K+ channel in isolated spinal dorsal horn neurons of the rat. *Neurosci. Lett.* **170**:208–212.
21. Tator, C.H. 1995. Update on the pathophysiology and pathology of acute spinal cord injury. *Brain Pathol.* **5**:407–413.
22. Jansen-Olesen, I., Mortensen, C.H., El-Bariaki, N., and Ploug, K.B. 2005. Characterization of K(ATP)-channels in rat basilar and middle cerebral arteries: studies of vasomotor responses and mRNA expression. *Eur. J. Pharmacol.* **523**:109–118.
23. Seino, S. 1999. ATP-sensitive potassium channels: a model of heteromultimeric potassium channel/receptor assemblies. *Annu. Rev. Physiol.* **61**:337–362.
24. Aguilar-Bryan, L., Nelson, D.A., Vu, Q.A., Humphrey, M.B., and Boyd, A.E., 3rd. 1990. Photoaffinity labeling and partial purification of the beta cell sulfonylurea receptor using a novel, biologically active glyburide analog. *J. Biol. Chem.* **265**:8218–8224.
25. Haseloff, R.F., et al. 2006. Differential protein expression in brain capillary endothelial cells induced by hypoxia and posthypoxic reoxygenation. *Proteomics.* **6**:1803–1809.
26. Wang, X., et al. 2004. Mechanisms of hemorrhagic transformation after tissue plasminogen activator reperfusion therapy for ischemic stroke. *Stroke.* **35**:2726–2730.
27. Chan, T.K., Chan, V., Teng, C.S., and Yeung, R.T. 1982. Effects of gliclazide and glibenclamide on platelet function, fibrinolysis and metabolic control in diabetic patients with retinopathy. *Sem. Hop.* **58**:1197–1200.
28. Rivlin, A.S., and Tator, C.H. 1977. Objective clinical assessment of motor function after experimental spinal cord injury in the rat. *J. Neurosurg.* **47**:577–581.
29. Nikulina, E., Tidwell, J.L., Dai, H.N., Bregman, B.S., and Filbin, M.T. 2004. The phosphodiesterase inhibitor rolipram delivered after a spinal cord lesion promotes axonal regeneration and functional recovery. *Proc. Natl. Acad. Sci. U. S. A.* **101**:8786–8790.
30. Basso, D.M., Beattie, M.S., and Bresnahan, J.C. 1995. A sensitive and reliable locomotor rating scale for open field testing in rats. *J. Neurotrauma.* **12**:1–21.
31. Hansen, A.M., et al. 2002. Differential interactions of nateglinide and repaglinide on the human beta-cell sulphonylurea receptor 1. *Diabetes.* **51**:2789–2795.
32. Stephan, D., Winkler, M., Kuhner, P., Russ, U., and Quast, U. 2006. Selectivity of repaglinide and glibenclamide for the pancreatic over the cardiovascular K(ATP) channels. *Diabetologia.* **49**:2039–2048.
33. Yokoshiki, H., Sunagawa, M., Seki, T., and Sperelakis, N. 1999. Antisense oligodeoxynucleotides of sulfonylurea receptors inhibit ATP-sensitive K+ channels in cultured neonatal rat ventricular cells. *Pflugers Arch.* **437**:400–408.
34. Sharma, N., et al. 1999. The C terminus of SUR1 is required for trafficking of KATP channels. *J. Biol. Chem.* **274**:20628–20632.
35. Galderisi, U., Cascino, A., and Giordano, A. 1999. Antisense oligonucleotides as therapeutic agents. *J. Cell. Physiol.* **181**:251–257.
36. Simard, J.M., Kent, T.A., Chen, M., Tarasov, K.V., and Gerzanich, V. 2007. Brain oedema in focal ischaemia: molecular pathophysiology and theoretical implications. *Lancet Neurol.* **6**:258–268.
37. Oertel, M., et al. 2002. Progressive hemorrhage after head trauma: predictors and consequences of the evolving injury. *J. Neurosurg.* **96**:109–116.
38. Gidday, J.M., et al. 2005. Leukocyte-derived matrix metalloproteinase-9 mediates blood-brain barrier breakdown and is proinflammatory after transient focal cerebral ischemia. *Am. J. Physiol. Heart Circ. Physiol.* **289**:H558–H568.
39. Noble, L.J., Donovan, F., Igarashi, T., Goussev, S., and Werb, Z. 2002. Matrix metalloproteinases limit functional recovery after spinal cord injury by modulation of early vascular events. *J. Neurosci.* **22**:7526–7535.
40. Pannu, R., Christie, D.K., Barbosa, E., Singh, I., and Singh, A.K. 2007. Post-trauma Lipitor treatment prevents endothelial dysfunction, facilitates neuroprotection, and promotes locomotor recovery following spinal cord injury. *J. Neurochem.* **101**:182–200.
41. Sun, H.S., Feng, Z.P., Barber, P.A., Buchan, A.M., and French, R.J. 2007. Kir6.2-containing ATP-sensitive potassium channels protect cortical neurons from ischemic/anoxic injury in vitro and in vivo. *Neuroscience.* **144**:1509–1515.
42. Merola, A., et al. 2002. Histologic characterization of acute spinal cord injury treated with intravenous methylprednisolone. *J. Orthop. Trauma.* **16**:155–161.
43. Faden, A.I., Lemke, M., Simon, R.P., and Noble, L.J. 1988. N-methyl-D-aspartate antagonist MK801 improves outcome following traumatic spinal cord injury in rats: behavioral, anatomic, and neurochemical studies. *J. Neurotrauma.* **5**:33–45.
44. Colak, A., et al. 2003. Neuroprotective effects of GYKI 52466 on experimental spinal cord injury in rats. *J. Neurosurg.* **98**:275–281.
45. Schwartz, G., and Fehlings, M.G. 2001. Evaluation of the neuroprotective effects of sodium channel blockers after spinal cord injury: improved behavioral and neuroanatomical recovery with riluzole. *J. Neurosurg.* **94**:245–256.
46. Teng, Y.D., et al. 2004. Minocycline inhibits contusion-triggered mitochondrial cytochrome c release and mitigates functional deficits after spinal cord injury. *Proc. Natl. Acad. Sci. U. S. A.* **101**:3071–3076.
47. Partridge, C.J., Beech, D.J., and Sivaprasadarao, A. 2001. Identification and pharmacological correction of a membrane trafficking defect associated with a mutation in the sulfonylurea receptor causing familial hyperinsulinism. *J. Biol. Chem.* **276**:35947–35952.
48. Nelson, D.A., Bryan, J., Wechsler, S., Clement, J.P., 4th, and Aguilar-Bryan, L. 1996. The high-affinity sulfonylurea receptor: distribution, glycosylation, purification, and immunoprecipitation of two forms from endocrine and neuroendocrine cell lines. *Biochemistry.* **35**:14793–14799.
49. Bracken, M.B., et al. 1990. A randomized, controlled trial of methylprednisolone or naloxone in the treatment of acute spinal-cord injury. Results of the Second National Acute Spinal Cord Injury Study. *N. Engl. J. Med.* **322**:1405–1411.
50. Choudhri, T.F., Hoh, B.L., Solomon, R.A., Connolly, E.S., Jr., and Pinsky, D.J. 1997. Use of a spectrophotometric hemoglobin assay to objectively quantify intracerebral hemorrhage in mice. *Stroke.* **28**:2296–2302.
51. Lorrain, J., et al. 2003. Antithrombotic properties of SSR182289A, a new, orally active thrombin inhibitor. *J. Pharmacol. Exp. Ther.* **304**:567–574.
52. Sumii, T., and Lo, E.H. 2002. Involvement of matrix metalloproteinase in thrombolysis-associated hemorrhagic transformation after embolic focal ischemia in rats. *Stroke.* **33**:831–836.
53. Gerzanich, V., et al. 2003. Alternative splicing of cGMP-dependent protein kinase I in angiotensin-hypertension: novel mechanism for nitrate tolerance in vascular smooth muscle. *Circ. Res.* **93**:805–812.